AIAA JOURNAL
Vol. 43, No. 12, December 2005

Computation of Actuation Power Requirements for Smart Wings with Morphing Airfoils

Frank H. Gern,* Daniel J. Inman,† and Rakesh K. Kapania‡
Virginia Polytechnic Institute and State University, Blacksburg, Virginia 24061

New generations of highly maneuverable aircraft, uninhabited combat air vehicles or micro air vehicles, are likely to feature very flexible lifting surfaces. To enhance the performance and control characteristics of these vehicles, the replacement of hinged control surfaces by smart wings with morphing airfoils is investigated. This requires a fundamental understanding of the interaction between aerodynamics, structures, and control systems. The modeling of a smart wing with morphing airfoils is described. Trailing-edge flaps for maneuvering are replaced by airfoil morphing via distributed structural actuation. The goal is to build a model consistent with distributed control and to exercise this model to determine the progress possible in terms of flight control (lift, drag, and maneuver performance) with an adaptive wing. The model is used to study the roll performance and actuation power requirements of a smart wing with morphing airfoils. For selected flight conditions, actuation power requirements of a smart wing with morphing airfoils are compared to those of a conventional wing with trailing-edge flaps.

Introduction

In general, owing to increased requirements for weight savings, aircraft structures are becoming more flexible, whereas their performance requirements are becoming more stringent. This is especially true for uninhabited combat air vehicles (UCAV) or micro air vehicles. Recently, a great effort has been put forth in designing "smart wings" for uninhabited as well as conventional aircraft. Smart wings as used here refer to the use of various active materials such as shape memory alloys, piezoceramics, electrostrictives, microelectromechanical systems, etc., to bend, twist, and change the surface of a wing in flight. This way, it becomes possible to obtain more favorable lift and drag properties, replace flaps or ailerons, prevent aeroelastic instabilities, and increase vehicle performance.

However, it appears that it is not known what level of performance is possible, what the loads are, or in general, how an adaptive wing would make a difference over conventional designs. This is especially the case when conventional, hinged control surfaces are to be replaced by morphing airfoils. A major question to be answered is whether a vehicle without hinged control surfaces will be able to create sufficient control authority to meet the stringent maneuverability requirements posed on new generations of air vehicles.

This project evaluates the performance of a smart wing as compared to a baseline wing with control surfaces. The effectiveness of a smart wing can be measured in terms of required time constants, forces, moments, and control power requirements to obtain maneuverability and performance characteristics similar or superior to those of a conventional wing. Various models of a generic adaptive wing at different levels of sophistication and their behavior under various control schemes are examined.

Received 26 September 2002; accepted for publication 21 June 2004.

*Research Assistant Professor, Department of Mechanical Engineering, Center for Intelligent Material Systems and Structures; currently Manager, New Business Development, Avionics Specialties, Inc., Charlottesville, VA 22906-6400. Senior Member AIAA.

†George R. Goodson Professor and Director, Department of Mechanical Engineering, Center for Intelligent Material Systems and Structures. Associate Fellow AIAA.

‡Professor, Department of Aerospace and Ocean Engineering. Associate Fellow AIAA.

Several adaptive wing programs have been conducted in research laboratories and by major airframe manufacturers (see, e.g., Refs. 1–3). UCAV with adaptive wings, i.e., without conventional flaps or vertical control surfaces, potentially offer enhanced stealth properties and reduced radar signature, thus increasing penetration into enemy airspace and lethality without putting human pilots at risk.

Project Overview and Objectives

The overall program goal is the determination of the minimum control energy required to increase the maneuverability and performance of a flapless UCAV by using smart structures and morphing airfoil technology. The program objectives are to determine the boundaries of adaptive wing performance by addressing the following goals[4]:

1) Mimic the effects of wings with conventional, discrete control surfaces. This will establish a comparison baseline for the performance evaluation of smart wings with morphing airfoils.

2) Determine the actuation energy, forces, moments, displacements, and time constants that are required of smart actuators to achieve the maneuverability and performance of air vehicles with conventional control surfaces by using morphing wings, i.e., wings that will change their shape but have no control surfaces. Ultimately, this will enable one to determine the control power depending on the maneuverability and/or vehicle performance.

3) Investigate the use of distributed actuation/control devices to i) enhance the maneuverability of a highly flexible wing and ii) increase the performance of the vehicle by expanding its flight envelope and/or its adaptability to different, often contrary mission requirements (multimission vehicle).

To meet the objectives, a multidisciplinary project team has been established. The team consists of three major task forces: dynamics and control, aeroservoelasticity, and adaptive structures (Fig. 1).

The adaptive structures work focuses on the structural and aeroelastic modeling of a generic flexible UCAV wing/fuselage configuration. The model allows a refined analysis of the wing structure featuring spars, ribs, and skins. It incorporates distributed internal actuation and can be easily adapted to changes in the structural configuration. This model is being used as a platform to study the influence of distributed sensing/actuating and morphing airfoils on flight performance. It is completely validated by finite element analyses. The present paper summarizes the main features of this model and describes recent findings regarding morphing wing actuation power requirements.

The dynamics and control work studies morphing airfoils in steady and unsteady flow and innovative strategies to control the aircraft by using wing morphing. Special attention is given to the

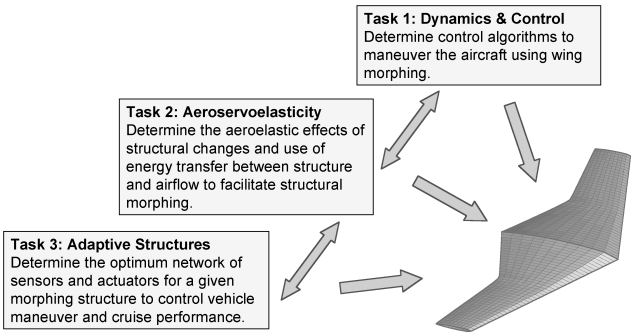

Fig. 1 Project tasks and their interaction.

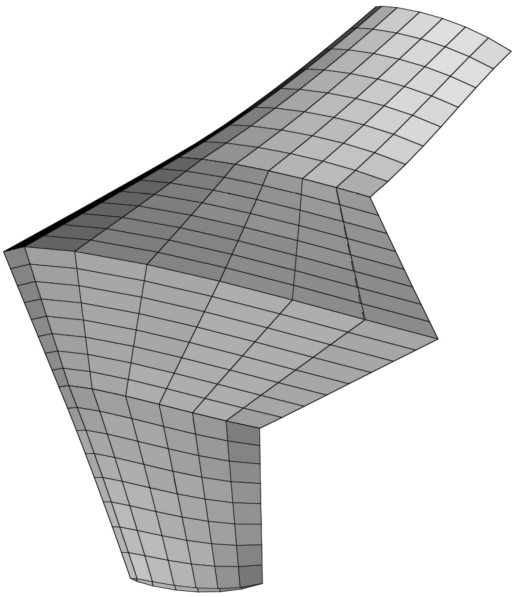

Fig. 2 Generic UCAV vehicle with lambda wing and morphing airfoil sections.

three-dimensional interaction of pitch, yaw, and roll control in the absence of vertical control surfaces. A six-degree-of-freedom rigid-body flight simulator featuring a vehicle with morphing airfoils has been implemented and is being validated by finite element simulations.

The aeroservoelasticity work investigates aeroelastic effects of structural changes and the possibility of energy transfer between structure and airflow to facilitate structural morphing. One aspect of the aerodynamics work in this task is the drag prediction of morphing airfoils to create yawing moments sufficient to provide yaw control without vertical control surfaces. By using innovative morphing airfoil concepts, the potential of shape changes to create yawing moments in the order of magnitude of vertical control surfaces or split rudders is investigated.

Structural and Aerodynamic Modeling

For the structural analyses, an equivalent plate model of a generic flying-wing-type UCAV configuration has been developed (Fig. 2). A detailed description of the representation of the different structural wing elements (skins, spars, and ribs) used with this model can be found in Refs. 4 and 5. To model the special planform of the employed lambda wing geometry, two trapezoidal plates have to be joined. To find the static aeroelastic response of the lambda wing and to study the influence and effectiveness of different actuation shemes, the aerodynamic loads are calculated based on the vortex lattice method (VLM). For this purpose, a linearized compressible VLM code has been used. A detailed description of the aerodynamic load calculation can be found in Ref. 6.

To account for compressibility effects, the airflow density is corrected according to the freestream Mach number by using the Prandtl–Glauert correction. The flow tangency boundary condition is formulated to consider the spanwise variation of the sectional pitch and dihedral, as well as the chordwise variation of the airfoil camber surface, and therefore accounts for rigid and flexible components. For accurate prediction of the aerodynamic loads, both the inboard and outboard wing sections have been subdivided into a lattice of 10 chordwise and 10 spanwise equally spaced vortex panels, yielding a total of 200 vortex panels for half of the vehicle. The control point of the bound vortex has been fixed at the $\frac{3}{4}$ chord position of each panel.

Model Validation

The structural and aeroelastic models have been validated by using the finite element package MSC/NASTRAN. The finite element calculations are made with 238 structural nodes and 848 elements. The wing skins are modeled as shell elements (CQUAD4), the spar and rib caps are represented as bar elements (CBAR), and the spar and rib webs are modeled by using shear panel elements (CSHEAR). For the aeroelastic analysis in NASTRAN, the lambda wing has been modeled as two interfering lifting surfaces. Both inboard and outboard wing sections have been subdivided into 10 chordwise and 10 spanwise aerodynamic panels, yielding a total number of 200 aerodynamic boxes for one half of the vehicle and providing an aerodynamic modeling similar to the one applied with the equivalent plate analysis. The aerodynamic loads are calculated using the doublet lattice method for the flight conditions given earlier. A detailed assessment of the validation results is presented in Ref. 5.

Distributed Structural Actuation

A distributed structural actuation scheme has been implemented to obtain any desired twist or camber deformation of the wing structure. For the specific vehicle under investigation, the inboard wing section/fuselage is relatively rigid. Therefore, only the outboard section of the wing is assumed to be fully adaptive. The inboard wing/fuselage section foresees actuation of the trailing edge for high lift generation and gust load alleviation (Fig. 3). Distributed actuation of the outboard wing can be achieved by placing actuators at the spanwise rib stations. More radical concepts may even completely remove the ribs or foresee adaptive ribs for morphing the airfoil (see, e.g., Ref. 5).

To analyze the deformation behavior of this structural actuation scheme by using the equivalent plate model, the individual actuator forces are being replaced by the equivalent moments they create within the wing structure. So far, no assessment has been made concerning an optimization of the actuator distribution or an optimum structural wing configuration to minimize actuation energy and required actuator power (structural flexibility tailoring). The actual realization of such a distributed structural actuation scheme will require further assessment in the future.

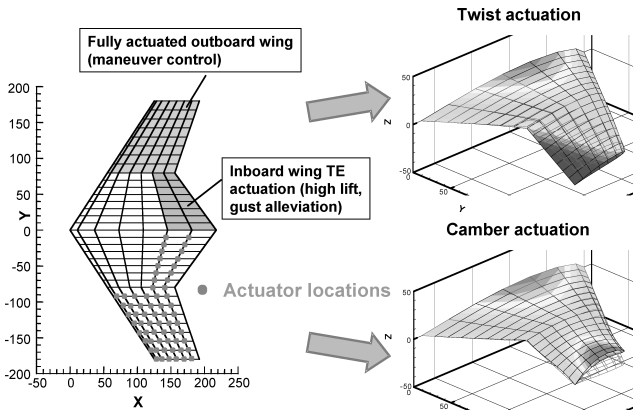

Fig. 3 Distributed structural actuation and resulting wing deformations.

Activation of the actuators in a way that all of the resulting moments are of the same sign, i.e., producing a torque in the same direction, will enable one to twist the wing in either direction, trailing edge up or down. If the resulting moments near the leading and trailing edge of the wing are of opposite signs, the camber shape of the airfoil can be modified. Therefore, based on the input from the flight control system, any desired combination of wing twist and camber actuation can be realized for maneuver control of the vehicle.

Figure 3 further depicts two possible twist and camber deformations of the wing resulting from the described distributed actuation scheme. To outline the basic effects, the actuator force has been kept constant at all actuator locations, varying only the signs of the moments to produce twist or camber actuation. To induce significant wing deformations for illustrative purposes, a relatively high actuator force of 10,000 lb (44,482 N) has been assumed, creating a twist rotation of 13 deg at the wing tip. Much smaller deformations and actuator forces are expected for maneuver control of the vehicle.

The distributed structural actuation scheme has been validated by using NASTRAN. Wing deformations obtained from NASTRAN agree within 8% (twist actuation) and 1% (camber actuation) with those obtained from the equivalent plate model.[7]

Roll Performance

Figure 4 depicts the calculated pressure distribution on the investigated UCAV vehicle for 0-, 5-, and 10-deg antisymmetrically deflected trailing-edge flaps at reference conditions {dynamic pressure 782.8 lb/ft^2 [5.436 psi (37.48 kPa)], corresponding to a Mach number of 0.728 and a dive speed of 553 mi/h (247.2 m/s) at sea level[8]}. The significant pressure spike at the leading edge of the flap is typical due to the sharp change in the downwash distribution of the lifting surface and has been well described in the literature. The twist moment created by this increased lift near the trailing edge untwists the wing at higher dynamic pressures, therefore causing reduced aileron effectiveness and roll reversal. For the morphing wing, a c_L increase equivalent to that obtained from a flap deflection is achieved by modification of the airfoil camber and twist by using the distributed actuation scheme described earlier. The wing morphing is calibrated to yield the same c_L increase as the 5- and 10-deg deflected flaps at reference conditions.

As can be seen from Fig. 5, omitting hinged control surfaces promises improvements in the aerodynamic quality of the wing. The pressure distribution of the smart wing does not exhibit the pressure spike of a hinged flap. Furthermore, the absence of sharp edges and deflected surfaces reduces radar signature and visibility of the vehicle, thus enhancing its stealth properties.

As a measure of smart wing effectiveness, roll performance has been investigated by several authors.[1,2,9] Figure 6 compares the rolling moment vs dynamic pressure obtained for a wing with trailing-edge flaps to that of a morphing wing for different actuation schemes. As can be seen from Fig. 6, the roll performance and roll reversal characteristics highly depend on the nature of the actuation scheme.

For comparison purposes, the wing morphing is calibrated to yield a rolling moment equivalent to a 15-deg flap deflection at reference conditions. Compared to the trailing-edge flap, twist actuation offers the possibility of high roll performance for higher flight speeds; however, roll performance of a twist actuated morphing wing is relatively poor for lower flight speeds. The major advantage of twist actuation is the elimination of roll reversal. This is because aerodynamic loads on the wing are shifted toward the leading edge, thus supporting additional wing twist and avoiding the washout effects that cause roll reversal. As mentioned before, the deflection of trailing-edge flaps is shifting aerodynamic loads toward the trailing edge, thus promoting washout and decreasing aileron effectiveness for higher dynamic pressures and, finally, roll reversal.

An important conclusion that can be drawn from Fig. 6 is that morphing wings do not necessarily have to improve roll performance by simply omitting trailing-edge flaps. Pure camber actuation yields an even lower roll reversal speed than the trailing-edge flap. This is due to an out-of-plane bending of the wing during camber actuation, which increases the washout effect and therefore reduces the reversal speed. However, compared to a twist-actuated wing, the camber actuated wing offers higher roll performance in the low-speed regime.

The real power of the morphing wing concept lies in its ability to continuously cover the entire region of roll performance from pure camber actuation to pure twist actuation without requiring structural modifications. Instead, the roll performance of the wing may simply be tailored by employing different control laws and actuation schemes. This suggests the implementation of complex control laws with adaptive actuation schemes according to the actual flight conditions, thus allowing exploitation of the full potential of wing morphing throughout the flight envelope of the vehicle.

Actuation Energy and Power Requirements

One of the most important issues and concerns in smart wing technology has been the actuation energy and power that have to be provided by the vehicle's onboard power system. Naturally, a smart wing may almost always require the deformation of some, preferably secondary, wing structure with the actual power requirements heavily depending on the wing structural realization and actuation scheme. Here one of the major advantages of a flap becomes obvious, as the presence of a hinge line allows the actuation energy to be kept to a minimum. Nevertheless, this hinge line usually causes problems under certain flight conditions in terms of flow separation and blow-through effects, thus significantly reducing the actual flap effectiveness as compared to theoretical results.[10] For the present study, actuation energy and power of the trailing-edge flap have

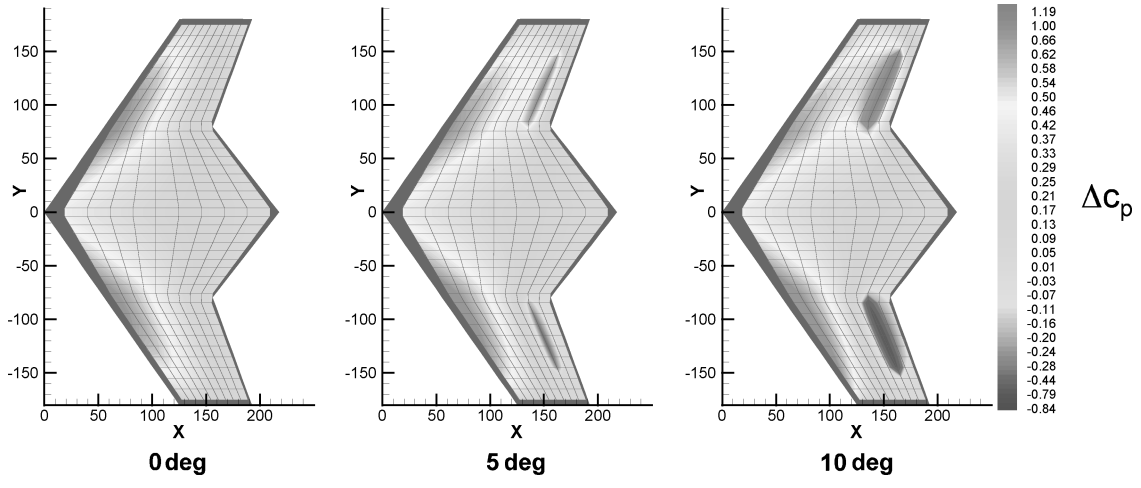

Fig. 4 Aerodynamic pressure coefficient distribution on a generic UCAV for different trailing-edge flap deflection angles.

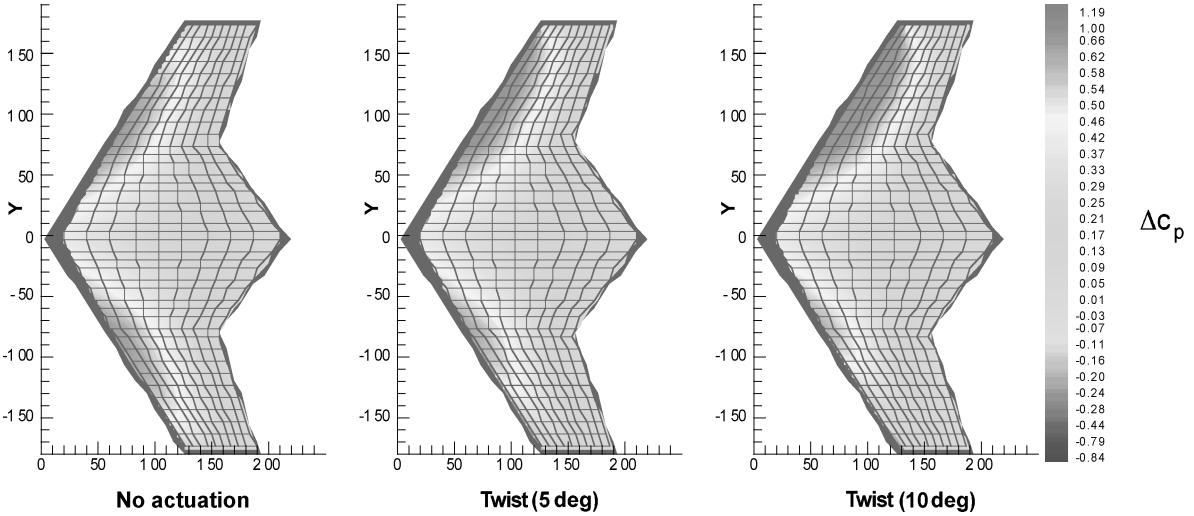

Fig. 5 Aerodynamic pressure coefficient distribution on a generic UCAV for twist actuation equivalent to different trailing-edge flap deflection angles.

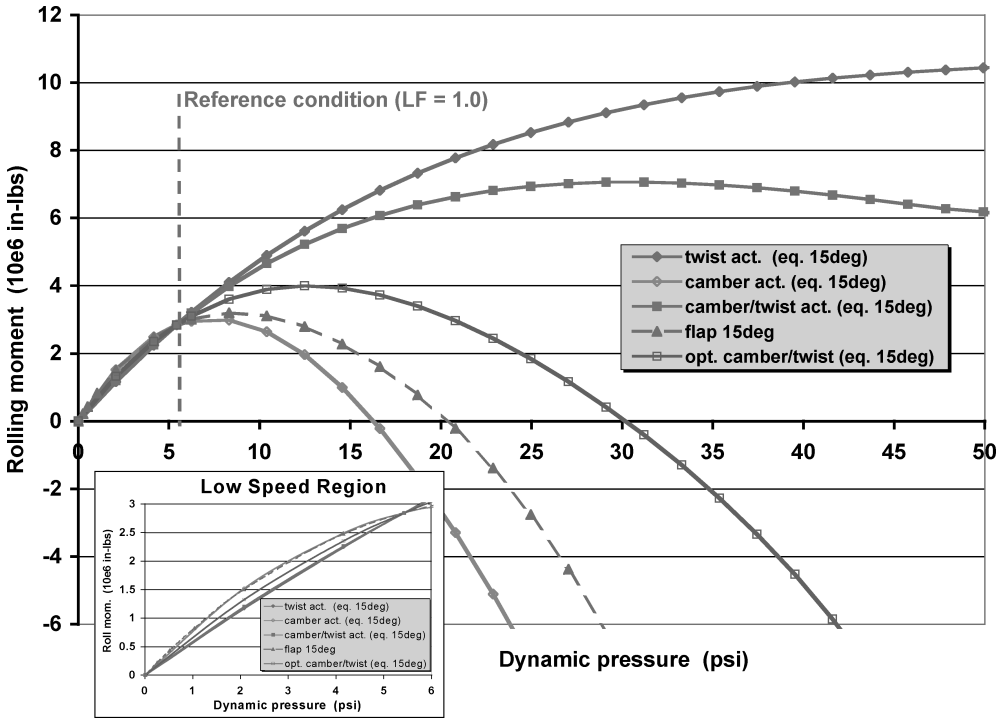

Fig. 6 Comparison of roll performance vs flight dynamic pressure for the wing with trailing-edge flaps and morphing wing with different actuation schemes.

been calculated on the basis of the work performed by the flap in the aerodynamic flowfield. Assuming the rotation of the flap to be around a hinge line at the flap's leading edge, the actuation energy of the flap can be simply expressed as

$$\Delta W_{\text{flap}} = \int_0^{\delta} M_{\text{flap}}(\delta)\,\mathrm{d}\delta$$

$$= \sum_{\text{flap panels}} \int_0^{\delta} \Delta S_{\text{flap panel}} q\,\Delta c_p(\delta) x_{\text{flap panel}}\,\mathrm{d}\delta \qquad (1)$$

In Eq. (1), ΔW_{flap} is the flap actuation energy, M_{flap} is the flap hinge moment, and δ is the flap deflection angle. The flap hinge moment is obtained by summing the aerodynamic forces acting on the individual flap panel areas ΔS, multiplied by their respective moment arms $x_{\text{flap panel}}$; q is the dynamic pressure, and Δc_p is the effective pressure coefficient of the respective panel. The flap actuation power is calculated based on the assumption of a 90-deg/s flap angular rotation velocity, which is a typical value for primary control surfaces of high-performance fighters.

Figure 7 depicts the flap actuation power vs flight dynamic pressure required to produce a rolling moment equivalent to that obtained by a 5-deg antisymmetrical flap deflection at reference conditions [950,000 in. · lbf (107,336 Nm)]. As expected, the actuation power for the upward-deflecting flap (left wing) is much lower than for the downward-deflecting flap (right wing). This is because the motion of the upward-deflected flap reduces the sectional wing lift and is supported by the aerodynamic forces. The downward-deflecting flap increases the lift by performing work against the aerodynamic force field. The total actuation power increases with increasing dynamic pressure, tending toward infinity close to the aileron reversal speed, at which the aileron effectiveness rapidly decreases to zero.

To accurately assess the actuation energy and power requirements for the morphing wing, all three energy quantities associated with

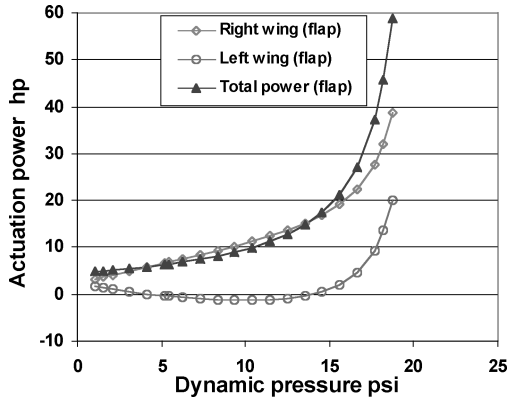

Fig. 7 Actuation power vs flight dynamic pressure for the wing with trailing-edge flaps. The rolling moment created is equivalent to the one obtained by a 5-deg antisymmetrical flap deflection at reference conditions [950,000 in. · lbf (107,336 Nm)].

the morphing wing structure in the aerodynamic flowfield have been computed by using their respective structural and aerodynamic representations. The wing structure's strain energy has been computed from the equivalent plate model as described in Refs. 4 and 5 and is given by

$$U = \frac{1}{2}\iiint_{v} \{\sigma\}^T\{\varepsilon\}\,\mathrm{d}V = \frac{1}{2}\{q\}^T[K]\{q\} \tag{2}$$

In Eq. (2), U is the strain energy, V is the volume occupied by all of and only the structural components of the wing, σ is the stress vector, and ε is the strain vector. By performing the transformations described in Ref. 11, the strain energy can also be computed from the generalized displacement vector q and the wing stiffness matrix K.

The work performed by the aerodynamic forces during the wing morphing is calculated from the employed VLM:

$$\Delta W_{\text{aero}} = \sum_{\text{aero panels}} \int_0^x \Delta S_{\text{aero panel}} q\,\Delta c_p(x)\,\mathrm{d}x \tag{3}$$

In Eq. (3), ΔW_{aero} is the total work performed by the aerodynamics, ΔS is the area of the individual aerodynamic panels, q is the dynamic pressure, Δc_p is the effective pressure coefficient of the respective panel, and x is the displacement of the respective panel.

The work performed by the distributed actuators is computed from the actuator moments M_{actuator} and the respective rotation θ of each actuator:

$$\Delta W_{\text{actuators}} = \sum_{\text{actuators}} \int_0^{\theta} M_{\text{actuator}}\,\mathrm{d}\theta \tag{4}$$

To compare the actuation power requirements of the morphing wing to the baseline wing with trailing-edge flaps, the rolling moment created by the morphing wing was calibrated to be identical to that produced by the trailing-edge flaps in Fig. 7 [950,000 in. · lbf (107,336 Nm)]. Furthermore, the required wing deformation is assumed to occur within the same time span, i.e., equivalent to a 90-deg/s flap rotation. Figure 8 depicts the actuation power for a morphing wing with twist actuation vs the dynamic pressure. In contrast to the wing with flaps (dashed line for reference), the actuation power of the morphing wing decreases with increasing flight speed, reflecting the increasing roll performance of this actuation scheme. Because the twist actuated wing does not exhibit roll reversal, there is no dramatic increase in the actuation power at higher flight speeds. However, in the low-speed regime, the required actuation power is very high, as the low dynamic pressure requires high structural deformations to create the desired rolling moment. The employed actuation power computation scheme assumes prescribed actuator moments and wing deformations. As a result, actuation powers computed for the left and right wings are identical.

Table 1 Different energy quantities computed for the morphing wing with twist actuation at reference conditions[a]

Quantity	Unit	Right wing	Left wing
Strain energy	in. · lbf	11,503.0	1,074.3
Aerodynamic work	in. · lbf	5,763.3	−4,572.1
Actuation energy	in. · lbf	5,660.6	5,657.1
Actuation power (90 deg/s)	in. · lbf/s	8,506.1	8,500.8
	hp	15.5 (flap 6.8)	15.4 (flap −0.45)

[a]Dynamic pressure 782.8 lb/ft^2 [5.436 psi (37.48 kPa)], corresponding to a Mach number of 0.728 and a dive speed of 553 miles/h (247.2 m/s) at sea level.[8] The wing deformation is calibrated to yield a rolling moment equivalent to a 5-deg antisymmetrical trailing-edge flap deflection.

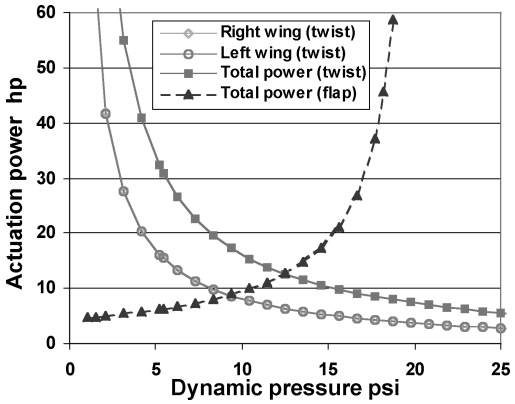

Fig. 8 Actuation power vs flight dynamic pressure for the morphing wing with twist actuation. The rolling moment created is equivalent to that obtained by a 5-deg antisymmetrical flap deflection at reference conditions [950,000 in. · lbf (107,336 Nm)]. Actuation power for left and right wings is identical.

To highlight the accuracy of the actuation power calculations for the morphing wing, Table 1 shows the energy quantities computed at reference conditions. Although all of the quantities are calculated from the different models with different grid points and integration schemes according to Eqs. (2–4), the actual numbers for strain energy, aerodynamic work, and actuation energy show good agreement. Table 1 shows that the actuation energy required by the morphing wing is not simply the strain energy in the structure but is given by the difference between the strain energy and the work performed by the aerodynamic forces. As a result, further efforts on minimizing the actuation energy should focus on employing the aerodynamics in the most beneficial way; in other words, let the aerodynamics help as much as possible to deform the wing. As an example, for the current nonoptimum actuation scheme, the actuation energy on the left wing is almost completely consumed by the work of the aerodynamic forces, whereas on the right wing both aerodynamics and actuators deform the wing. This suggests that unsymmetrical actuation schemes, in which most of the work is performed on the right wing, might create the same roll performance with less actuation power. A detailed assessment of this possibility is the subject of ongoing investigations.

Table 1 indicates that for the investigated case, the required total actuation power for both left and right wings for the morphing wing is about five times the value of the wing with trailing-edge flaps. However, for the wing with flaps, this actuation power usually has to be provided by a single actuator, whereas in the current study, the actuation power to morph the wing is generated by a field of 48 actuators per wing. This reduces the power that has to be provided per actuator to only about 0.3 hp. For redundancy reasons, a conventional flap generally is connected to at least one or two additional actuators to provide sufficient flight control in case of airframe damage or actuator failure, which might dramatically increase the power actually "carried" by a vehicle with conventional

control surfaces. As an example, "the flight control actuation system [of the B-2 Stealth Bomber] includes 24 actuators . . . At least two actuators drive each of the 11 primary control surfaces. Each actuator is powered by two different hydraulic systems so that each control surface is connected to all four hydraulic systems. The centerline [gust load alleviation surface] (GLAS) is the only exception and is plumbed to only two hydraulic systems."[12]

In contrast to this, it is anticipated that a morphing wing with its heavily distributed actuation will provide sufficient robustness and redundancy to account for actuator failures without carrying a complete backup system for each single actuator. Preliminary studies with single or even multiple actuator failures showed only small increases in the required actuation power to create the desired roll performance.

In this context, it should be mentioned that the actuation energy and power requirements obtained so far employ only a generic actuation scheme, assuming that all actuators create similar moments. Optimizing the location, stroke, and moment of each individual actuator poses a typical multidisciplinary design optimization problem with the actuation energy or actuation power as an objective function to minimize. In a similar way, the wing structure itself may by optimized to exhibit the desired flexibility for a reduced actuation effort when needed, and yet to provide sufficient rigidity when required to sustain the high load factors of future air vehicles (structural flexibility tailoring).

Conclusions

Smart wings with morphing airfoils offer great potential for increasing the performance of future air vehicles. The paper outlined the possibility of increasing the roll performance of a smart wing with distributed actuation over a conventional wing with trailing-edge flaps. The roll-reversal behavior of the smart wing can be tailored by simply changing the actuation scheme in the flight controls while maintaining the same structural setup. This becomes an important strategy as the maximum of roll performance for different actuation schemes occurs at different flight speeds. Intelligent controllers are required to adaptively modify the control laws according to the actual flight conditions to provide the desired vehicle performance throughout the flight envelope.

Distributed actuation offers great potential in terms of system robustness and is anticipated to account for sufficient controllability in case of airframe damage or actuator failure. Further work is required concerning the minimization of actuation energy and actuation power by optimizing actuator locations, strokes, and moments. Tailoring the flexibility of the wing structure of a morphing wing offers additional potential for minimizing the actuation power.

Acknowledgments

This project is sponsored by the Air Force Office of Scientific Research and DARPA under Grant F49620-99-1-0294, with Brian Sanders and Ephrahim Garcia as Technical Monitors. The authors also thank their team members Harry Robertshaw, Greg Pettit, Anand Natarajan, and Erwin Sulaeman for the valuable discussions and contributions.

References

[1]Khot, N. S., Appa, K., Ausman, J., and Eastep, F. E., "Deformation of a Flexible Wing Using an Actuating System for a Rolling Maneuver Without Ailerons," AIAA Paper 98-1802, April 1998.

[2]Chen, P. C., Nam, C. H., Sarhaddi, D., Liu, D. D., Griffin, K., Heeg, J., and Yurkovich, R., "Torsion-Free Wing Concept for Enhanced Aircraft Maneuver," AIAA Paper 2000-0223, April 2000.

[3]Powers, S. G., Webb, L. D., Friend, E. L., and Lokos, W. A., "Flight Test Results From a Supercritical Mission Adaptive Wing with Smooth Variable Camber," NASA TM-4415, NASA Dryden Flight Research Facility, Edwards, CA, Aug. 1992.

[4]Inman, D. J., Robertshaw, H. H., Kapania, R. K., and Gern, F. H., "Distributed Modeling and Control of Adaptive Wings," DARPA/Air Force Office of Scientific Research, Rept. F49620-99-1-0294, Sept. 2000.

[5]Gern, F. H., Inman, D. J., and Kapania, R. K., "Structural and Aeroelastic Modeling of General Planform UCAV Wings with Morphing Airfoils," *AIAA Journal*, Vol. 40, No. 4, 2002, pp. 628–637.

[6]Gern, F. H., Sulaeman, E., Naghshineh-Pour, A., Kapania, R. K., and Haftka, R. T., "Structural Wing Sizing for Multidisciplinary Design Optimization of a Strut-Braced Wing," *Journal of Aircraft*, Vol. 38, No. 1, 2001, pp. 154–163.

[7]Inman, D. J., Gern, F. H., Robertshaw, H. H., and Kapania, R. K., "Comments on Prospects of Fully Adaptive Aircraft Wings," *Proceedings of SPIE*, Vol. 4332, edited by A.-M. R. McGowan, Society of Photo-Optical Instrumentation Engineers (International Society for Optical Engineering), Bellingham, WA, 2001, pp. 1–9.

[8]Bisplinghoff, R. L., Ashley, H., and Halfman, R. L., *Aeroelasticity*, Addison Wesley, Cambridge, MA, 1955, p. 467.

[9]Pendleton, E., Bessette, D., Field, P., Miller, G., and Griffin, K., "The Active Aeroelastic Wing Flight Research Program," *Journal of Aircraft*, Vol. 37, No. 4, 2000, pp. 554–561.

[10]Sanders, B., and Eastep, F. E., "Aerodynamic Improvements with Conformal Control Surfaces," *Advances in Computational Engineering and Sciences*, Vol. 2, edited by S. N. Atluri and F. W. Brust, Tech Science Press, Palmdale, CA, 2000.

[11]Kapania, R. K., and Liu, Y., "Static and Vibration Analyses of General Wing Structures Using Equivalent-Plate Models," *AIAA Journal*, Vol. 38, No. 7, 2000, pp. 1269–1277.

[12]Britt, R. T., Jacobson, S. B., and Arthurs, T. D., "Aeroservoelastic Analysis of the B-2 Bomber," *Journal of Aircraft*, Vol. 37, No. 5, 2000, pp. 745–752.

M. Ahmadian
Associate Editor